10. Compressive Strength of Long Rectangular Plates under Hydrostatic Pressure

Hiroo OKADA*, *Member*, Koichi OSHIMA**, *Member*
and Yoshio FUKUMOTO*, *Member*

(From J.S.N.A. Japan, Vol. 146, Dec. 1979)

Summary

In this paper, the compressive strength of long rectangular plates (aspect ratio $\alpha=3$ and $\alpha=4$) under increasing compression and constant hydrostatic pressure, is studied theoretically and experimentally as a basic study on the compressive strength of a ship's bottom plating. The theoretical calculations are performed by following two methods assuming that the plate behaves elastically up to the collapse.

a) The method assuming that the plate collapses when the normal stress in the direction of compression at the longitudinal edges of the plate will become equal to yield stress of the material.

b) The method assuming that the plate collapses when the plate will satisfy the condition of plastic collapse based on plastic analysis in which collapse mechanism is assumed and the large deformation theory is considered.

From these results of theoretical calculations and experiments, conclusion is summarized as follows:

(1) The compressive strength for comparatively thin plates having the large value of $(b/t)\sqrt{\sigma_Y/E}$ where collapse of the plate will occur in postbuckling state does not change so much with hydrostatic pressure, while for comparatively thick plates having the small value of $(b/t)\sqrt{\sigma_Y/E}$ where collapse of the plate will occur in prebuckling state, the compressive strength changes remarkably with hydrostatic pressure.

(2) Calculated values of the compressive strength based on the method a) are generally larger than those based on the method b). The difference of the two becomes more remarkable for thicker plates having the small value of $(b/t)\sqrt{\sigma_Y/E}$ under larger hydrostatic pressure.

(3) Experimental results of this study concerning thin plates having comparatively large values of $(b/t)\sqrt{\sigma_Y/E}$ agree generally with the tendency of theoretical results.

1. Introduction

In this paper, the compressive strength of simply supported long rectangular plates (aspect ratio $\alpha=3$ and 4) under edge thrust and constant lateral pressure is investigated theoretically and experimentally, as a basic study on the compressive strength of a ship's bottom plating.

Many studies have been made of the ultimate strength of plate structures under compression. For examples, H. Otsubo and Y. Ueda studied that of square plates[1),2)], and also Y. Ueda et al studied that of stiffened plates[3)] by means of the FEM, respectively. As studies by means of analytical methods, studies have been made of the ultimate strength of stiffened plates under compression[4)] and of square plates

* University of Osaka Prefecture
** Graduate Student of University of Osaka Prefecture

under compression and shear[5] by Y. Fujita et al, and studies have been also made of the ultimate strength of wide plates[6] and stiffened plates under compression[7),8] by H. Otsubo et al. The autors have also studied the buckling strength of long rectangular plates under compression and hydrostatic pressure by means of analytical methods[9]. And in this paper, by using above results, they study the compressive strength of plates under such combined loads. Calculations are performed by means of following two methods assuming that the plates behaves elastically up to the collapse; a) the method assuming that the plate collapses when the normal stress in the direction of compression at the longitudinal edges of the plate becomes equal to yield stress of the material and b) the methods assuming that the plate collapses when the plate satisfies the condition of plastic collapse based on plastic analysis. From these results, the effect of lateral pressure on the compressive strength of the plates is discussed. Furthermore, comparison between experimental results performed for thin plates and theoretical results mentioned above is also made.

2. The Elastic Behaviours of Simply Supported Long Rectangular Plates under Edge Thrust and Lateral Pressure

2.1 The Analytical Methods

We consider the elastic behaviour of a simply supported long rectangular plates ($a \times b \times t$) having comparatively large aspect ratio $\alpha(\equiv a/b)$, subjected to increasing edge thrust p and constant lateral pressure q.

Such a plate deflects due to lateral pressure q from the beginning as shown in Fig. 1 (b). When longitudinal compression p is added, the amount of deformation will increase but type of deformation will remain in the form of one half-wave until p reaches the buckling load. When p reaches the buckling load, type of deformation will change rapidly and take a form of several half-waves as shown in Fig. 1 (c). (Number of half-waves is determined by aspect ratio α). Such behaviours of the plate are pursued by means of the following method, i.e., the deflection of the plate is assumed including unknown constants, and they are determined by means of energy method. And here, all edges of the plate are assumed to be kept straight after deformation, as in-plane boundary condition.

The coordinate system O-xyz is taken as in Fig. 1.

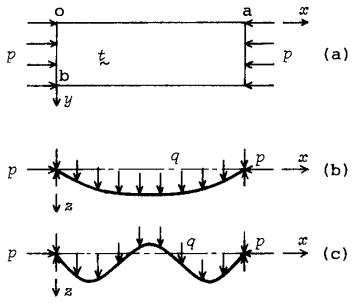

Fig. 1 Long rectangular plates under compression and hydrostatic pressure

The basic equations governing the large deflection behaviour of rectangular plates with flexural rigidity D and Young's modulus E under such combined loads may be stated as:

$$\nabla^4 F = E(w_{,xy}^2 - w_{,xx} w_{,yy}) \tag{1}$$

$$\nabla^4 w = q/D + (t/D)(F_{,yy} w_{,xx} + F_{,xx} w_{,yy} - 2F_{,xy} w_{,xy}) \tag{2}$$

where F is the Airy's stress function defining the in-plane mid-surface stress and where w is the deflection of the plate and ∇^4 the well-known bi-harmonic operator. In these equations a comma followed by subscripts represents partial differentiation in turn with respect to each subscript. Eq. (1) represents the compatibility equation and eq. (2) represents the out-of-plane equilibrium equation.

Here, considering the boundary conditions and deformation of the plate before and after buckling, w is assumed to take a form as

$$w=\sum_{n=1}^{N} w_n \sin\frac{n\pi}{a}x \sin\frac{\pi}{b}y \qquad (3a)$$

where w_n $(n=1,2, \ldots, N)$ are unknown constants and N is approximately determined according to aspect ratio α of the plate as follows:

$$N=3 \text{ for } \alpha=3 \text{ and } N=4 \text{ for } \alpha=4 \qquad (3b)$$

The stress function F containing unknown constants w_n is obtained by substituting eq. (3) into eq. (1), satisfying the relevant conditions.

Subsequently, we determined the unknown constants by using the principle of stationary potential energy, that is, $\delta\phi=0$, instead of the equilibrium equation (2). ϕ is expressed by

$$\phi=U+V \qquad (4)$$

where U is given by the sum of the strain energy U_b due to bending deformation and the strain energy U_m due to in-plane deformation, and V is given by the potential due to p and q. ϕ is obtained as a function of the unknown constants w_n by substituting w and F into eq. (4). Consequently, the unknown constants w_n are determined by $\delta\phi=0$, that is,

$$\frac{\partial\phi}{\partial w_n}=0 \quad (n=1, 2, \cdots, N) \qquad (5)$$

The equilibrium configuration of the system is thus determined by above eq. for given p and q (this concrete expression is shown in Appendix A).

Besides, the stability of the equilibrium configuration being determined by the sign of $\delta^2\phi$, the stable condition is given by $\delta^2\phi>0$, that is,

$$\phi_{11}>0, \quad \begin{vmatrix}\phi_{11} & \phi_{12}\\ \phi_{12} & \phi_{22}\end{vmatrix}>0, \cdots, \quad \begin{vmatrix}\phi_{11} & \phi_{12} & \cdots & \phi_{1N}\\ & \phi_{22} & & \vdots\\ \text{SYM.} & & \ddots & \\ & & & \phi_{NN}\end{vmatrix}>0 \qquad (6)$$

where $\phi_{ij}=\partial^2\phi/\partial w_i \partial w_j$

2.2 The Elastic Behaviours and Buckling Phenomena

(a) Simply supported rectangular plates of $\alpha=3$

In this article, the case of simply supported plates of $\alpha=3$ is considered. Behaviours of such plates are represented by applying $N=3$ at eq. (3)[9]. Numerical calculations are performed based on eqs. (5) and (6).

The curves showing the relation between edge thrust and the deflection of the plate are given schematically, in Fig. 2 in which stable paths are shown by full lines and unstable paths by broken lines. As seen from this diagram, there are two typical deformation patterns according to the magnitude of q.

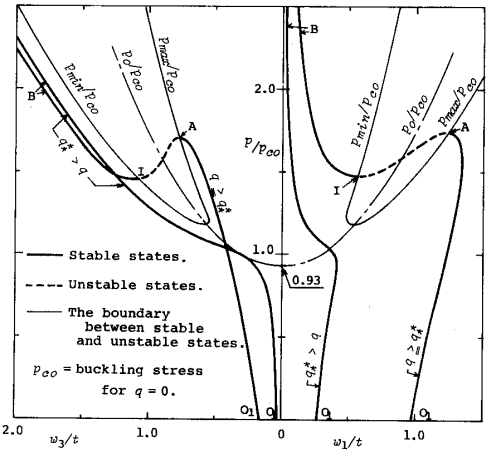

Fig. 2 $p/p_{CO}-w_1/t, w_3/t$ curves ($\alpha=3$)

(i) When the lateral pressure q is small $(q\leqq q_*^*=3.70Et^4/b^4)$.

In this case, the buckling does not occur in a strict sense of term; i.e., there is neither the bifurcation point nor the unstable paths on the edge thrust-deflection curves. But the deformation varies continuously towards the deflection form of triple bulges with the large value of w_3, with an increase of the edge thrust from the defection form of single bulge. Here, the load p_0 at which

the deflection at the center of the plate becomes zero (i.e., the load at $w_1=w_3$) is taken as the approximate value of the buckling load from the practical point of view.

(ii) When the lateral pressure q is large ($q_*^* \leqq q$).

The buckling occurs at a certain edge thrust (say p_{max} (the load at the point A in Fig. 2)). In this case, the deformation shows 'jump phenomenon', from the deflection form of a single bulge with the large value of w_1 (the curve O_1A) to the deflection form of triple bulges with the large value of w_3 (the curve IB), at $p = p_{max}$.

Moreover, in this case, there are two stable paths within certain limits below the buckling load (say $p_{max} \geqq p \geqq p_{min}$ (the load at the minimum point I)) as seen from Fig. 2. Therefore, there exists the possibility of occurrence of jump phenomenon at the limits of these loads, under the stimulus of external disturbances. Then, besides the buckling load p_{max} , the load at the lower limit p_{min} is taken as critical load from the practical point of view.

In the case of $\alpha=3$, there exist the deformations of $w_2 \neq 0$ in large values of p, but their paths are unstable.

The values of p_{max} , p_{min} and p_0 show increasing tendency according to the increase of q (the diagram is omitted (see Ref. 9)).

(b) Simply supported rectangular plates of $\alpha=4$

Behaviours of simply supported rectangular plates of $\alpha=4$ are represented by applying $N=4$ at eq. (3)[9].

The curves showing the relation between the edge thrust and the deflection are given schematically, in Fig. 3 in which only stable paths having high degree of the stability are shown by full lines considering energy criterion for stability. As seen from this diagram, the deformation patterns are divided into two main groups according to the magnitude of q.

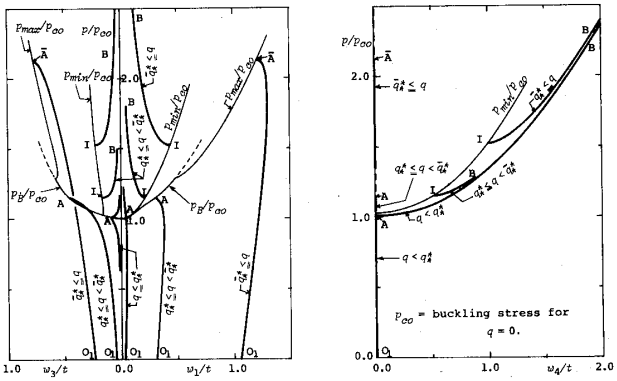

Fig. 3 $p/p_{CO} - w_1/t$, w_3/t and w_4/t curves ($\alpha = 4$) ($p/p_{CO} - w_2/t$ curves are omitted.)

(i) When the lateral pressure is small ($q \leqq q_*^* = 0.47 Et^4/b^4$).

The buckling occurs at a certain edge thrust (say p_B (the load at the point A in Fig. 3)). In this case, the deformation changes continuously, from the deflection form of a single bulge with the large value of w_1 (the curve O_1A) to the deflection form of quadruple bulges with the large value of w_4 (the curve IB) with an increase of the edge thrust; here, p_B corresponds to the bifurcation point of edge thrust-deflection curves (Fig. 3).

(ii) When the lateral pressure is large ($q_*^* \leqq q$).

The deformations show always jump phenomena in this case; the type of deformation is subdivided into two neglecting stable paths with low degree of the stability.

a) In case of $q_*^* \leqq q \leqq \bar{q}_*^*$ ($\bar{q}_*^* = 3.56\, Et^4/b^4$) The buckling occurs at a certain edge thrust (say p_B (the load at the bifurcation point A)). In this case, the deformation changes rapidly from the deflection form of a single bulge with the large value of w_1 (O_1A curve) to the deflection form of quadruple bulges with the large value of w_4 (IB curve).

b) In case of $\bar{q}_*^* \leqq q$: The buckling occurs at a certain edge thrust (say p_{max} (the load at the maximum point $\bar{A}$)). In this case, the deformation changes also

rapidly from the deflection form of a single bulge with the large value of w_1($O_1\bar{A}$ curve) to the deflection form of quadruple bulges with the large value of w_4 (IB curve).

Moreover, in these cases a) and b) stated above, there are two states of stable paths within certain limits below the buckling laod (say $p_B \geqq p \geqq p_{min}$ (the load at the minimum point I) for the case of a), $p_{max} \geqq p \geqq p_{min}$ (the load at the minimum point I) for the case of b)) as seen from Fig. 3. Therefore, there exists the possibility of occurrence of jump phenomenon at the load beyond p_{min} under the stimulus of external disturbances. From the practical point of view, besides the buckling loads p_B and p_{max}, the load at the lower limit p_{min} is also taken as a critical load.

The relation between p_B, p_{max} and p_{min} and q is shown in Fig. 5 or Fig. 8. These curves have increasing tendency as q increase similar to the case of $\alpha=3$.

3. The Compressive Strength of Simply Supported Long Rectangular Plates under Hydrostatic Pressure

3.1 The Analytical Methods

Here, let us consider the compressive strength of simply supported long rectangular plates of aspect ratio $\alpha=3$ and 4 under edge thrust and lateral pressure. To obtain the ultimate strength of these plates strictly, the relation between load and deflection must be pursued by considering the extent of yielding area of the plate due to loads. This may be obtained by using the FEM or the FSM which was developed in recent years. However, these methods require a long computer processing time, and are not always effective for discussing the behaviours of the plate qualitatively.

Then, in this chapter we evaluate the compressive strength approximately by following two methods assuming that the plate behaves elastically up to the collapse. In the first method, it is assumed that the plate fails when the normal stress $|\sigma_r|$ in the direction of compression at the longitudinal edges of the plate becomes equal to yield stress σ_Y of the material. In the second method, it is assumed that the plate fails when it satisfies the condition of plastic collapse based on the plastic analysis in which collapse mechanism is assumed and the large deflection theory is considered[4),5)].

Hereafter, leading the equations which define the condition of the collapse of the plate, the compressive strength based on these equations is calculated and the effect of lateral pressure on the compressive strength is also discussed from above results.

(a) The method assuming that the plate collapses when the normal stress at the longitudinal edges reaches the yield stress.

Assuming that the plate behaving as calculated by eqs. (5) and (6) for given q collapses at the moment the edge stress $-\sigma_r$ reaches yield stress σ_Y, the compressive strength p_u is defined by the load which satisfies the following condition

$$-\sigma_r=\frac{Et^2}{b^2}\left[\frac{\pi^2}{3(1-\nu^2)}\frac{p}{p_{c0}}+4\pi^2\sum_{n=0}^{2N}\bar{B}_n\cos\frac{n\pi}{a}x_0\right]=\sigma_Y \tag{7}$$

where x_0 is the value which makes left hand side of eq. (7) maximum. p_{c0} is the buckling stress for $q=0$ and $\bar{B}_n$ is shown in Appendix A. From above eq. and eq. (5), the compressive strength p_u and the values of $w_1 \sim w_N$ are determined.

(b) The method assuming that the plate collapses when it satisfies the condition of the plastic collapse

Carrying out the plastic analysis in which collapse mechanism is assumed and the large deflection theory is considered, the compressive strength of the plate is calculated as the load at which the deformation of the plate obtained by elastic analyses satisfies the condition of the plastic collapse.

Let us show the condition of the plastic

collapse in which the large-deflection is considered. It is assumed that the material of the plate is the perfectly rigid plastic body following the von Mises's yielding condition and that the plastic hinge lines are straight. Based on these assumptions, the following equation is given by the principle of virtual work considering the large-deflection of the plate.

$$\sum_{m=1}^{r}\int_{l_m}(M_p+wN)\delta\Theta\, dl_m=\int_0^a\int_0^b q\,\delta w\,dx\,dy \qquad (8)$$

where N: the in-plane tensile force per unit width on the plastic hinge lines of the plate

M_p: the full plastic moment per unit width considering the effect of in-plane force on the plastic hinge lines of the plate

w: the deflection of the plate

$\delta\Theta$: the angular variation of the plastic hinge of the plate due to the virtual deflection δw

l_m: the m-th plastic hinge line

r: number of the plastic hinge lines

Using eq. (8) for typical collapse modes of the plate under such combined loads, the conditions of the plastic collapse are expressed as follows:

(A) When the collapse mode having k long hip-roofs of the same type in a series (refer to Fig. 4 (a)) is assumed $(k<\alpha)$

$$\{m_{45}+(\alpha/k-1)m_0/2-Aqb^4/(Et^4)\}/\mu=w_B/t \qquad (9a)$$

where,

$$A=\begin{cases}0 & (k:\text{even})\\ (3\alpha/k-1)/\{12k\sigma_Y b^2/(Et^2)\} & (k:\text{odd})\end{cases}$$

$$\mu=p/\sigma_Y$$

$$m_{45}=4(1-\mu^2)/\sqrt{16-15\mu^2}$$

$$m_0=2(1-\mu^2)/\sqrt{4-3\mu^2}$$

(B) When the collapse mode having k regular pyramids of the same type in a series (refer to Fig. 4 (b)) is assumed ($k=\alpha$, α: integer).

$$\{m_{45}-Bqb^4/(Et^4)\}/\mu=w_B/t \qquad (9b)$$

where,

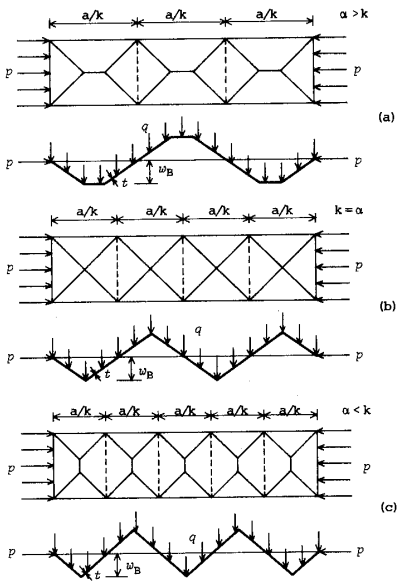

Fig. 4 Collapse modes of long rectangular plates with simply supported edges.

$$B=\begin{cases}0 & (k:\text{even})\\ 1/\{6k\sigma_Y b^2/(Et^2)\} & (k:\text{odd})\end{cases}$$

(C) When the collapse mode having k wide hip-roofs of the same type in a series (refer to Fig. 4 (c)) is assumed $(k>\alpha)$.

$$\{2m_{45}+(k/\alpha-1)m_{90}-Cqb^4/(Et^4)\}\div\{4\mu\times(k/\alpha-0.5)\}=w_B/t \qquad (9c)$$

where,

$$C=\begin{cases}0 & (k:\text{even})\\ \alpha(3-\alpha/k)/\{6k^2\sigma_Y b^2/(Et^2)\} & (k:\text{odd})\end{cases}$$

$$m_{90}=1-\mu^2$$

w_B in above eq. is the maximum deflection of the plate in the state of the collapse. The condition of the plastic collapse is obtained as the function of p and w_B for given q. Consequently, the compressive strength p_u and the values of $w_1\sim w_N$ are determined from eqs. (5) and (9).

3.2 The Compressive Strength

(a) The case based on the method a)

Numerical calculations are performed for the plate of aspect ratio $\alpha=3$ and 4. Fig. 5 shows the relation between p_u and q for the plate of $\alpha=4$ having the values of $b/t)\sqrt{\sigma_Y/E}=2.8$ (the thin plate) and

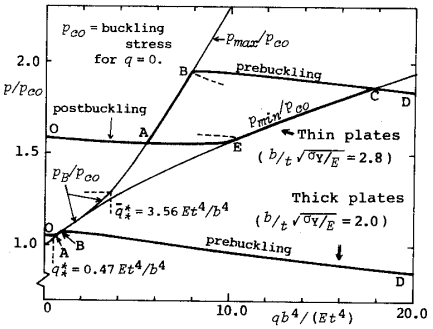

Fig. 5 $p_u/p_{co}-qb^4/(Et^4)$ curves for plates ($\alpha=4$) — method a) —

$b/t)\sqrt{\sigma_Y/E}=2.0$ (the comparatively thick plate) by using the $p_u/p_{co}-qb^4/(Et^4)$ coordinate. In this diagram, p_u is shown by heavy full lines and p_B, p_{max} and p_{min} which are buckling loads or its critical load stated in chapter 2 is shown by thin full lines. And here, the compressive strength concerning the stable paths with low degree of the stability are also omitted since they can be neglected for practical use.

As seen from this diagram, the compressive strength p_u and its deformation patterns vary according to the magnitude of q as follows.

In case of the thin plate $((b/t)\sqrt{\sigma_Y/E}=2.8)$, under small lateral pressure (corresponding to q between O and A), the plate collapses at a certain load p_u given by the curve OA after the buckling occurred at the load p_B or p_{max}. Under lateral pressure corresponding to q between A and B, at the moment buckling occurs at the load p_{max} (the curve AB) the plate collapses, i.e., $p_u=p_{max}$. Under lateral pressure beyond q given by the point B, the plate collapses at a certain load p_u given by the curve BCD before buckling. Therefore, p_u curve is given by OABCD in Fig. 5 under no external disturbances. However, under the stimulus of external disturbances, there exists the possibility of occurrence of jump phenomenon at the load beyond p_{min}. If buckling occurs at the load $p=p_{min}$, p_u curve will be given by AEC instead of ABC (in this case, the curve AE corresponds to the collapse after buckling, and the curve EC corresponds to the collapse at the moment of buckling). Therefore, p_u given by the curve OAECD may be considered the lower limit of the compressive strength from the practical point of view.

In case of the thick plate $((b/t)\sqrt{\sigma_Y/E}=2.0)$, the points corresponding to A and E, B and C in the case of the thin plate approaching each other, they can be considered to be centered at one point. Consequently, under small lateral pressure (corresponding to q between O and A), the plate collapses at a certain load p_u given by the curve OA after buckling. Under lateral pressure corresponding to q between A and B, the plate collapses at the moment buckling occurs at the load p_B, i.e., $p_u=p_B$. Under lateral pressure beyond q given by the point B, the plate collapses at the load p_u given by the curve BD before buckling.

In case of very thick plates, though the diagram is omitted, the curves corresponding to OA and AB stated above vanish, and the plate collapses always before buckling.

The tendency of the results obtained in the case of $\alpha=3$ is generally similar to those mentioned in the case of $\alpha=4$ (the diagram is omitted).

Fig. 6 and Fig. 7 show the relation between the compressive strength p_u and $(b/t)\sqrt{\sigma_Y/E}$ with various lateral pressure.

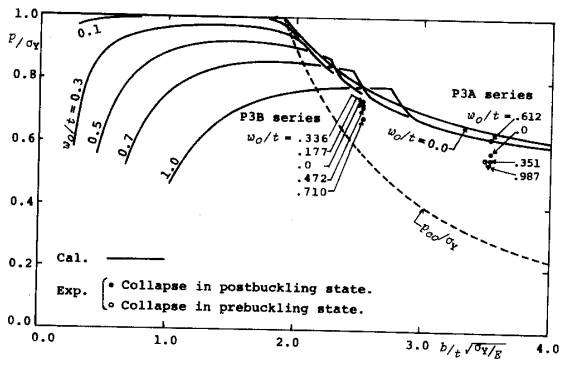

Fig. 6 $p_u/\sigma_Y-(b/t)\sqrt{\sigma_Y/E}$ curves for various values of w_0/t ($\alpha=3$) — method a) —

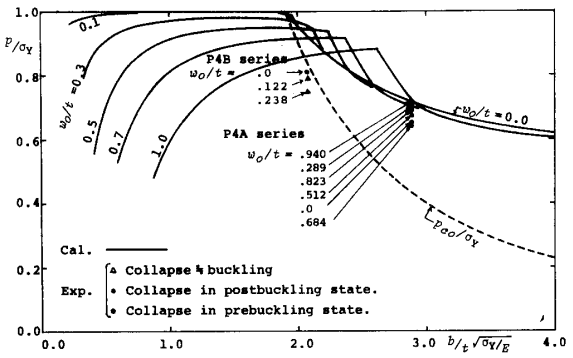

Fig. 7 $p_u/\sigma_Y-(b/t)\sqrt{\sigma_Y/E}$ curves for various values of w_0/t ($\alpha=4$) – method a) –

In these diagrams, w_0/t is used as the parameter instead of $qb^4/(Et^4)$, in which w_0 is the deflection at the center of the plate under lateral pressure alone. And as the values of p_u, the lower limits of the compressive strength are shown by considering the existence of external disturbances. Fig. 6 corresponds to the case of $\alpha=3$ and Fig. 7 corresponds to the case of $\alpha=4$.

It is seen from the both diagrams that in the thick plate the value of p_u/σ_Y decreases with increase of lateral pressure while in the thin plate the value of p_u/σ_Y does not change so much with lateral pressure. Moreover, in the case of intermediate value of $(b/t)\sqrt{\sigma_Y/E}$, there is the range where the value of p_u/σ_Y increases with increase of lateral pressure; this corresponds to the range where $p_u=p_{min}$.

(b) The case based on the method b)

In the calculations of the compressive strength p_u by using eqs. (5) and (9), the following case concerning the assumed collapse modes are investigated considering the elastic behaviours of the plate obtained in chapter 2.

(i) The case of $\alpha=3$: In case when the collapse of the plate occurs before buckling, the mode having one hip-roof type ($k=1$ in eq. (9a)) is assumed and as the maximum deflection of the plate w_B, mean deflection from the point $x=b/2$ to $x=a-b/2$ on the $y=b/2$ is adopted. In case when the plate collapses after buckling, the mode having three regular pyramids of the same type ($k=3$ in eq. (9b)) is assumed and w_3 is adopted as w_B.

(ii) The case of $\alpha=4$: In case when the plate collapses before buckling, both the mode having one hip-roof type ($k=1$ in eq. (9a); w_B is defined similarly in the case of $\alpha=3$) and the mode having three long hip-roofs of the same type ($k=3$ in eq. (9a); $w_B=w_3$) are assumed. In case when the plate collapses after buckling, the mode having four regular pyramids of the same type ($k=4$ in eq. (9b); $w_B=w_4$) is assumed.

Fig. 8 shows the relation between p_u and q for the plate of $\alpha=4$ having the values of $(b/t)\sqrt{\sigma_Y/E}=2.8$ and 2.0 by using the same coordinate as Fig. 5. In this diagram, the compressive strength concerning the stable paths with low degree of the stability is also omitted since they can be neglected for practical use. The values of p_B, p_{max} and p_{min} are plotted by the thin full lines. It is seen from this diagram that the compressive strength p_u and its collapse mode vary according to the magnitude of q as follows.

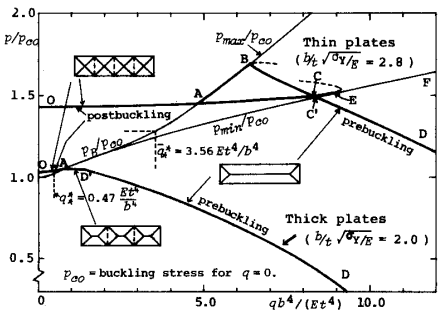

Fig. 8 $p_u/p_{c0}-qb^4/(Et^4)$ curves for plates ($\alpha=4$) – method b) –

In case of the thin plate ($(b/t)\sqrt{\sigma_Y/E}=2.8$), under small lateral pressure (corresponding to q between O and A), after buckling occurs at the load p_B or p_{max}, the plate collapses at a certain load p_u given by the curve OA with the mode of four regular pyramids type. Under lateral pressure corresponding to q between A and B, at the moment buckling occurs the plate

collapses in the case of no external disturbances, i.e., $p_u=p_{max}$. Under lateral pressure larger than q at the point of B, the plate collapses before buckling with the mode of one hip-roof type at the load p_u given by the curve BCD. In this case, the curve CE which represents p_u after buckling has not any mean as the collapse load. Therefore, p_u curve is given by OABCD under no external disturbances. However, according to the amount of external disturbances, under lateral pressure corresponding to q between A and C, the plate may collapse at the load p_u given by the curve AC after buckling occurred at the larger load than p_{min}, or at the load beyond AC at the moment buckling occurs. Therefore, under lateral pressure between A and C, p_u given by the AC curve is considered the lower limit of the compressive strength. While, under lateral pressure between C and C' (C' is the intersection of the curve BD and the curve p_{min}/p_{c0}), the collapse load after buckling due to external disturbances is larger than that before buckling, the p_u curve given by OACD is considered, as a whole, to be the lower limits of the compressive strength from the practical point of view.

In case of the comparatively thick plate ($(b/t)\sqrt{\sigma_Y/E}=2.0$), the points corresponding to A, B and C in the case of the thin plate approaching each other, they can be considered to be centered at a point. Then, under small lateral pressure the plate collapses at a certain load p_u given by the curve OA after buckling occurred at the load p_B. Under lateral pressure beyond q at the point A, the plate collapses always before buckling and there are two types of the collapse modes having the deflection form of triple bulges with the large value of w_3 (p_u is given by the curve AD') and the deflection form of a single bulge (p_u is given by the curve DD').

In case of very thick plate, though the diagram is omitted, curves corresponding to the part of OA and AD' stated above vanish, and the plate collapses always before buckling in deflection form of a single bulge.

As seen from this diagram, the compressive strength in the case when the plate will collapse after buckling does not change so much with lateral pressure, while the compressive strength in the case when the plate will collapse before buckling changes remarkably with lateral pressure. This tendency of the results obtained in the method b) is more remarkable as compared with that obtained in the method a).

Next, Fig. 9 and Fig. 10 show the relation between the compressive strength p_u and $(b/t)\sqrt{\sigma_Y/E}$ for various values of w_0/t using the same coordinate as Fig. 6 and 7. Considering the existence of external disturbances, the lower limits of the compressive strength are also taken as p_u. Fig. 9 corresponds to the case of $\alpha=3$ and Fig. 10 corresponds to the case of $\alpha=4$.

It is seen from the both diagrams that in the case of the thick plate the value of p_u/σ_Y changes remarkably with lateral pressure while in the case of the thin plate it does not change so much with lateral pressure.

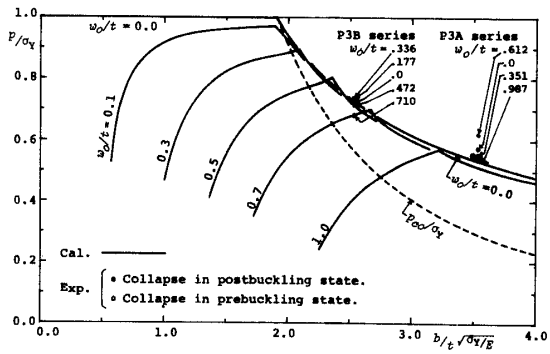

Fig. 9 $p_u/\sigma_Y-(b/t)\sqrt{\sigma_Y/E}$ curves for various values of w_0/t ($\alpha=3$ — method b) —

Moreover, the following conclusion is obtained from comparison the values of p_u based on the method a) with those based on the method b) using Fig. 6 and 9 and Fig. 7 and 10.

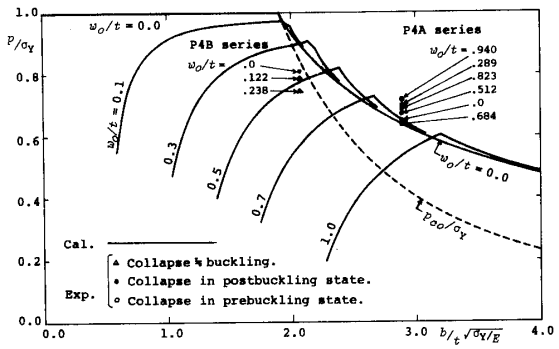

Fig. 10 $p_u/\sigma_Y-(b/t)\sqrt{\sigma_Y/E}$ curves for various values of w_0/t ($\alpha=4$) – method b) –

For the thin plate having the large value of $(b/t)\sqrt{\sigma_Y/E}$ where the plate will collapse after buckling, the variation of the calculated values of p_u/σ_Y based on the both methods due to lateral pressure is small. On the other hand, for the comparatively thick plate having small value of $(b/t)\sqrt{\sigma_Y/E}$ where the plate will collapse before buckling, this variation is large. The calculated values based on the method a) are generally larger than those based on the method b). The difference of the two for the range of small value of $(b/t)\sqrt{\sigma_Y/E}$ becomes more remarkable under larger lateral pressure.

4. The Experiments on Long Rectangular Plates under Compression and Lateral Pressure

4.1 The Experimental Method, Apparatus and Specimens

To verify the theoretical analyses on the behaviours and the compressive strength of the plate, we made a series of compressive experiments using a special apparatus as shown in Fig. 11, in which the longitudinal edges of a specimen are supported by the knife edges, and the upper and lower edges of the specimen are also supported by being caught in two plates. The lateral pressure is applied to the plate by air through a vynil bag leading to the air regulator as shown in Fig. 11(b). The upper and lower edges of the specimen are compressed being kept parallel by rigid frame. As shown in Fig. 11 (c), the longitudinal edges of the outside of knife edges are fitted with two tie plates to be kept straight after deformation.

The material of specimens used in this experiment is mild steel SS41 of 3mm and 4.5mm thick. The length and width of the specimen to be fitted with two tie plates are 1000mm and 380mm for the case of $\alpha=3$, 1000mm and 300mm for the case of $\alpha=4$, respectively; the width is larger than a space b between supported lines by knife edges (b=300mm ($\alpha=3$), b=250mm ($\alpha=4$)) by 25mm in each side and a space a between the upper and lower edges supported by two plates by length of 3mm is 994mm. The mechanical properties of the specimens are shown in the column (3) and (4) of Table 1.

4.2 The Experimental Results

We made a series of the compressive experiments varying systematically lateral pressure for the specimens having aspect ratio $\alpha=3$ and 4. The experimental conditions and the results and some data of load-deflection curves are shown in Table 1 and Fig. 12, 13, respectively.

Column (1) of Table 1 is name of a specimen: P3A series implies the specimen of the thin plate and $\alpha=3$, P3B series implies

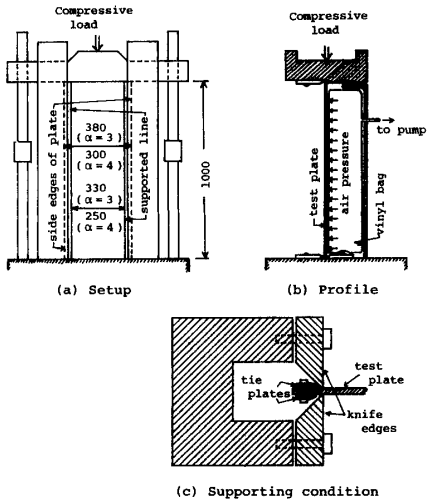

Fig. 11 Experimental apparatus

Table 1 Test conditions and results

	(1) Specimen	(2) Plate thickness t mm	(3) Young's modulus E kg/mm^2	(4) Yield stress σ_Y kg/mm^2	(5) $\frac{qb^4}{Et^4}$	(6) $\frac{w_0}{t}$	(7) Max. load ton	(8) Number of waves	(9) $\bar{J}=J/(bt^3)$	(10) Reduced $(p_u/\sigma_Y)_s$
	P3A-00	3.09	$\times10^4$ 2.10	25.4	0	0	17.5	3	$\times10^{-2}$ 6.14	0.574
	P3A-05				3.08	0.351	17.0	3		0.555
	P3A-10				6.16	0.612	18.8	3		0.622
	P3A-20				12.4	0.987	17.0	1		0.555
α=3	P3B-00	4.42	$\times10^4$ 2.19	27.4	0	0	34.4	3	$\times10^{-2}$ 3.57	0.726
	P3B-10				1.43	0.177	34.9	3		0.738
	P3B-20				2.85	0.336	35.0	3		0.740
	P3B-30				4.28	0.472	34.0	3		0.717
	P3B-50				7.24	0.710	32.6	1		0.683
	P4A-00	3.03	$\times10^4$ 2.05	29.1	0	0	18.5	4	$\times10^{-2}$ 8.43	0.653
	P4A-10				2.26	0.289	19.6	4		0.701
	P4A-20				4.52	0.512	19.0	4		0.675
	P4A-30				6.78	0.684	18.2	4		0.640
α=4	P4A-40				9.04	0.823	18.4	4		0.691
	P4A-50				11.3	0.940	19.9	1		0.715
	P4B-00	4.54	$\times10^4$ 2.01	33.1	0	0	37.7	4	$\times10^{-2}$ 4.55	0.810
	P4B-20				0.91	0.122	36.8	1→4		0.787
	P4B-40				1.83	0.238	35.2	1→4		0.746

the specimen of the thick plate and α=3 and so on. The last two figures of the name show the value of lateral pressure expressed by water column in dm units. Column (2) shows the mean plate thickness of the specimens with every series. Column (5) shows non-dimensional air pressure $qb^4/(Et^4)$. In column (6), w_0/t, that is, the calculated values of the center deflection of the plate due to lateral pressure alone, mentioned in chapter 3, is shown. Column (7) shows the maximum load obtained in this experiment. Column (8) shows number of halfwaves of the deflection form at the time of collapse. Moreover, the mark 1 → 4 in this column shows that the deformation changes rapidly from the deflection form of single bulge to the deflection form of quadruple bulges before and after collapse.

Fig. 12 and 13 plot the relation between the deflection at the center line of the specimen w (in mm) and the compressive load p (in ton) and in the left lower parts of these diagrams, the obtained deflection

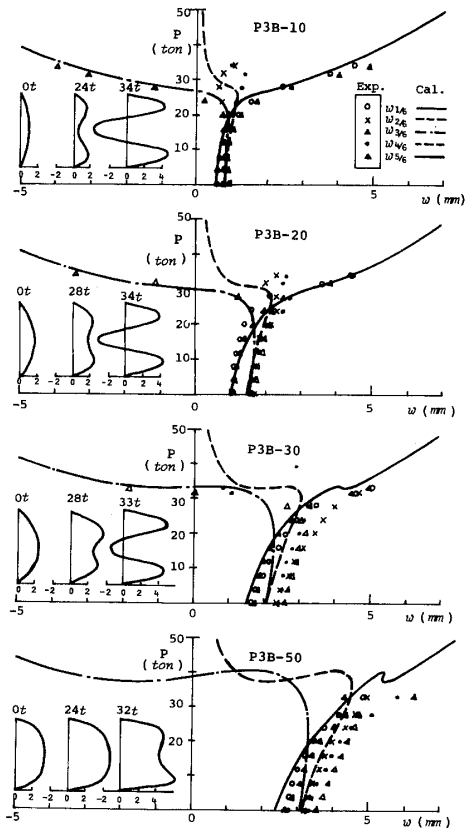

Fig. 12 Relation between compressive load and deflection (P3B series)

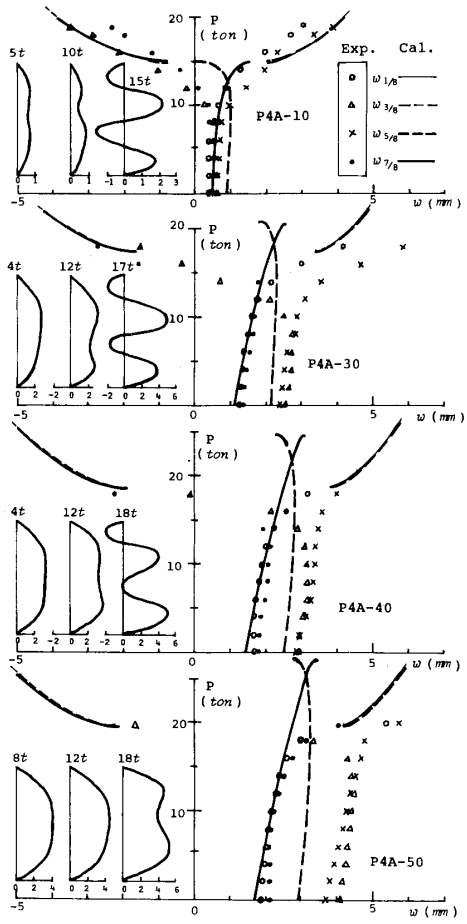

Fig. 13 Relation between compressive load and deflection (P4A series)

forms along the longitudinal center-line of the specimen for a few load steps are illustrated. Fig. 12 corresponds to the P3B series and Fig. 13 corresponds to the P4A series.

4.3 The Discussion on Theoretical Results

In this experiment, to keep the linearity of the deformation along the longitudinal edges of the specimen, these edges are fitted with two tie plates as stated before. Therefore, the rotational deformation of these edges is restricted to some extent by the torsional rigidity of this edge parts of the specimen. To estimate the behaviours and the compressive strengths of the specimens based on the calculated results for simply supported plates, it is necessary to convert calculated value as for p and σ_Y as follows

$$\left.\begin{aligned} p &\rightarrow p-\{6(1-\nu)\bar{J}\}p_{c0} \\ \sigma_Y &\rightarrow \sigma_Y-\{6(1-\nu)\bar{J}\}p_{c0} \end{aligned}\right\} \quad (10)^*$$

where, $\bar{J}=J/(bt^3)$ (refer to column (9) in Table 1)

J = the modulus of the torsional rigidity of the edge parts of the specimen

The curves described in Fig. 12 and 13 show the relation between the deflection and compressive load obtained by the above correction, corresponding to the experimental results. It is seen from the both diagrams that the experimental results are generally in good agreement with the calculated results including the jump phenomena except the range in which the plastic deformation of the plate dominates the behaviours (the vicinity of the compressive strength in the case of P3B-50 and P4A-50). The experimental results for the case other than P3B and P4A are also similar to above results.

Next, to compare the calculated results with the experimental results about the compressive strength, we convert the values of p_u/σ_Y obtained by these experiments into the values of $(p_u/\sigma_Y)_s$ corresponding to the calculated values for the simply supported plates shown in Fig. 6, 7, 9 and 10. The obtained results are shown in column (10) of Table 1 and are plotted in these diagrams. It is seen from these diagrams that the calculated values are comparatively in good agreement with the values of $(p_u/\sigma_Y)_s$ obtained by these experiments, though with a little scattering. Moreover, the experimental values are generally larger than the calculated values based on the method a) and smaller than those based on the method b) except the case of the P4B

* Though this correction is based on the calculation by the method a) cosidering the strain energy of the edge parts, similar conversion is also applied to the calculated results by the method b) approximately.

series. In the P4B series, it is supposed that since the edge parts of the specimen showed a tendency to go into inside when the deflection increased rapidly due to local plastic deformation, the experimental values of this series became generally small. As for the deflection forms at the time when the plate collapsed, the experimental results in the case where the plate collapsed after buckling correspond to the calculated results. Those in the case of P4B-20 and P4B-40 shown in column (8) of Table 1 with the mark 1 → 4, where the plate collapsed at the moment of buckling, correspond also to the calculated results. Those in the case of P3A-20, P3B-50 and P4A-50, where the plates collapsed before buckling, correspond comparatively to the calculated values based on the method b), and also correspond relatively to those based on the method a) except the case of P3A-20, considering that at its value of $(b/t)\sqrt{\sigma_Y/E}$ there exists the possibility of occurrence of collapse before buckling. Concerning P3A-20, correspondence of the calculated result by the method a) to the experimental result about the deflection form, is not good.

Moreover, the experiments were confined to the case of comparatively thin plates, since those for the case of the thick plate can not be made due to the limitation of the capacity of our testing apparatus.

5. Conclusion

As a basic research for the study of the strength of ship's bottom plating, the compressive strength of simply supported long rectangular plates under lateral pressure was approximately obtained by using the following two methods assuming that the plate behaved elastically up to collapse:

a) The method assuming that the plate collapses when the edge stress in the direction of compression becomes equal to yield stress of the material.

b) The method assuming that the plate collapses when it satisfies the condition of the plastic collapse in which collapse mechanism is assumed and the plastic large deflection theory is considered.

From these results, the effect of lateral pressure on the compressive strength was discussed. And at the same time, adequacy of the theoretical results was ascertained by experimental investigation. The obtained results are shown in the summary

Acknowledgment

The authors would like to express their sincere appreciation to Mr. K. Kitaura, Mr. Y. Taguchi, Mr. S. Watanabe, Mr. A. Ito and Mr. K. Hamada for their help in performing the experiments. A part of this work was supported by the Grant-in-Aid for Scientific Research of the Ministry of Education, Science and Culture of Japan. Furthermore, the numerical calculation in this paper was performed at the Data Processing Center, University of Osaka Prefecture.

Reference

1) H.OTSUBO; A Generalized Method of Analysis of Large-deformed Elastic-Plastic Plate Problems —Ultimate Strength of Compressive Plate with Initial Deflection—, J.SNA of Japan Vol. 130 (1971) (in Japanese)
2) Y.UEDA & others; Ultimate Strength of Square Plates Subjected to Compression (1st Report) —Effects of Initial Deflection and Welding Residual Stresses—, J. SNA of Japan Vol. 137 (1975) (in Japanese)
3) Y.UEDA, T.YAO & H.KIKUMOTO; Minimum Stiffness Ratio of a Stiffener against Ultimate Strength of a Plate, J.SNA of Japan Vol. 140 (1976) (in Japanese)
4) Y.FUJITA, T.NOMOTO & O.NIHO; Ultimate Strength of Stiffened Plates Subjected to Compression, J.SNA of Japan Vol. 141 (1977) (in Japanese)
5) Y.FUJITA, T.NOMOTO & O.NIHO; Ultimate Strength of Rectangular Plates Subjected to Combined Loading (1st Report), J.SNA of

Japan Vol. 145 (1979) (in Japanese)
6) H.OTSUBO, Y.YAMAMOTO & Y.J.LEE; Ultimate Strength of Wide Rectangular Plates, J.SNA of Japan Vol. 142 (1977) (in Japanese)
7) H.OTSUBO & others; Ultimate Compressive Strength of Stiffened Plates, J.SNA of Japan Vol. 143 (1978) (in Japanese)
8) Y.J.LEE, H.OTSUBO & Y.YAMAMOTO; Ultimate Compressive Strength of Stiffened Plates (2nd Report), J.SNA of Japan Vol. 144 (1978) (in Japanese)
9) H.OKADA, K.OSHIMA & Y.FUKUMOTO; A Basic Study on the Buckling Strength of a Ship's Bottom Plating, J.KSNA of Japan Vol. 173 (1979) (in Japanese)

Appendix A. The concrete expression of $\partial\phi/\partial w_n=0$ for the simply supported rectangular plate of aspect ratio α

$$\frac{12(1-\nu^2)}{\alpha^2}\left[2n^2\bar{B}_0\left(\frac{w_n}{t}\right)+\sum_{n-r\geq 1}\left\{-\frac{r^2}{2}\bar{A}_r+\left(n-\frac{r}{2}\right)^2\bar{B}_r\right\}\left(\frac{w_{n-r}}{t}\right)-\sum_{N\geq r-n\geq 1}\left\{-\frac{r^2}{2}\bar{A}_r+\left(n-\frac{r}{2}\right)^2\bar{B}_r\right\}\left(\frac{w_{r-n}}{t}\right)+\sum_{N\geq r+n}\left\{-\frac{r^2}{2}\bar{A}_r+\left(n+\frac{r}{2}\right)^2\bar{B}_r\right\}\left(\frac{w_{r+n}}{t}\right)\right]+\left\{\left(1+\frac{n^2}{\alpha^2}\right)^2-\left(\frac{p}{p_{c0}}\right)\left(\frac{n}{k}+\frac{kn}{\alpha^2}\right)^2\right\}\frac{w_n}{t}=\frac{192(1-\nu^2)}{\pi^6}\cdot\frac{1-\cos n\pi}{2n}\cdot\frac{qb^4}{Et^4} \qquad \text{(A1)}$$

where,

$$\bar{A}_0=0,\quad \bar{B}_0=\frac{1}{32\alpha^2}\sum_{n=1}^{N}n^2\left(\frac{w_n}{t}\right)^2$$

$$\bar{A}_n=\frac{\alpha^2}{4n^4}\left[\sum_{|k-l|=n}\sum(kl-k^2)\frac{w_kw_l}{t^2}+\sum_{k+l=n}\sum(kl+k^2)\frac{w_kw_l}{t^2}\right]$$

$$\bar{B}_n=\frac{\alpha^2}{4(n^2+4\alpha^2)^2}\left[\sum_{|k-l|=n}\sum(kl+k^2)\frac{w_kw_l}{t^2}+\sum_{k+l=n}\sum(kl-k^2)\frac{w_kw_l}{t^2}\right]$$

$p_{c0}=\pi^2D\{\alpha/k+k/\alpha\}^2/(tb^2)$: buckling stress for $q=0$, k = positive integer: number of half-waves of the deflection form at the moment of buckling

Appendix B. The full plastic Moment M_p considering the effect of inplane force

When the plate consisted of the perfectly rigid plastic body under compression p is bent at the plastic hinge line making the angle θ to the direction of the compression (refer to Fig. 14), the full plastic

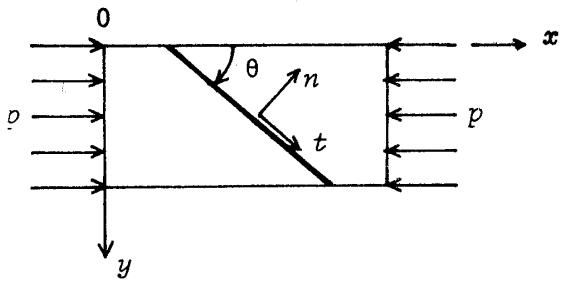

Fig. 14 Plastic hinge line of plate

moment M_p considering the effect of in-plane force acting the plate is obtained by considering the equilibrium of the in-plane force and von Mises's yielding condition as follows:

$$M_p/M_{p0}=2(1-\mu^2)/\sqrt{4(1-\mu^2)+\mu^2(2-3\cos^2\theta)^2}=m_\theta \qquad \text{(A2)}$$

where, $\mu=p/\sigma_Y$ and $M_{p0}=\sigma_Yt^2/4$: the full plastic moment without the effect of in-plane force. The values of m_θ for $\theta=45°$, 90° and 0° are given in eq. (9).